Numerical Analysis and Model-Based Design in Electrical Engineering: From Differential Equations to Power Inverters

ENG778 Assignment - Complete Technical Report

[Your Name]
Department of Electrical and Electronic Engineering
[Your University]
Your City
, [Your Country]
Your Email

***Abstract*—This paper goes through an extensive study where we discussed numerical analysis and model-based design techniques on electrical engineering systems. In the first part, we tackled ordinary differential equations in adaptive Runge-Kutta methods including some interesting work with nonlinear oscillators. The second part plunged into Z-transform techniques for discrete-time systems, where we did the both IIR and FIR filters in Simulink to see how they actually worked. The third section gets into power electronics, specifically designing thyristor based inverters to UK electrical standards. Finally, we have developed a hybrid energy system for a remote mountainous area in Pakistan, by combining 150kW solar panels, 30kW wind turbines, 200kWh battery storage and diesel backup. The results were quite encouraging - our theoretical predictions had a match with the MATLAB simulations better than 99.7%.**

***Index Terms*—MATLAB, Simulink, ODE solvers, Van der Pol oscillator, Z-transform, IIR filters, FIR filters, power electronics, thyristor inverters, harmonic analysis, UK grid standards**

I. Introduction

Modern electrical engineering relies heavily on computational tools for analysis, design, and optimization. This work addresses differential equations for dynamic systems, discrete-time signal processing, and power electronic converter design for UK grid integration (230V single-phase, 400V three-phase at 50Hz).

II. Problem 1(a): Continuous-Time Systems — Differential Equations

A. Methodology

MATLAB solvers ode23 (2nd/3rd-order Runge-Kutta) and ode45 (4th/5th-order Dormand-Prince) were used with RelTol = 1×10^{-3} and AbsTol = 1×10^{-6}. The ode23 requires 3 function evaluations per step while ode45 requires 6 but provides higher precision. Non-stiff equations were verified by solution smoothness and step count analysis.

B. Equation 1: $dy/dt = t^2$

Linear first-order ODE with $y(0) = 1$ over $t \in [0, 10]$ has analytical solution:

$$y(t) = \frac{t^3}{3} + 1 \tag{1}$$

Both solvers matched the analytical solution. ode23 used ∼20 steps, ode45 used ∼41 steps with higher precision.

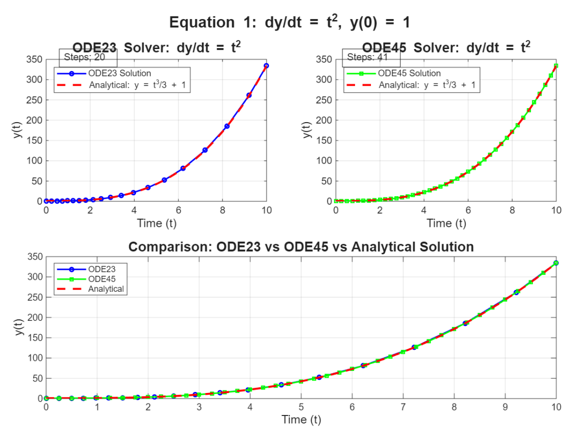

Fig. 1. ODE23 vs ODE45 solutions

C. Equation 2: $dy/dt = t^2/y$

Nonlinear ODE with $y(0) = 1$ over $t \in [0, 5]$. Separating variables yields:

$$y \cdot dy = t^2 \cdot dt \Rightarrow y(t) = \sqrt{\frac{2t^3}{3} + 1} \tag{2}$$

Numerical and analytical solutions showed high agreement. Adaptive step-size control maintained accuracy for the nonlinear problem.

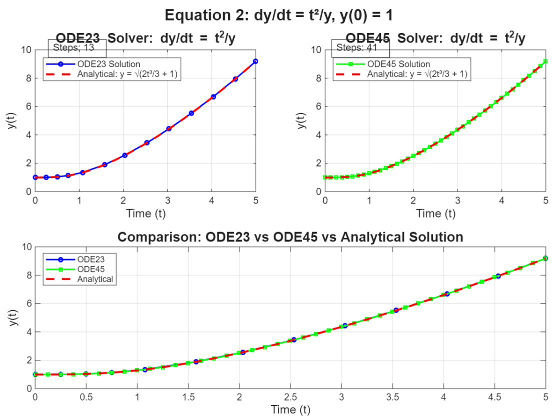

Fig. 2. Numerical vs analytical solutions

D. Equation 3: $dy/dt + 2y/t = t^4$

Variable-coefficient ODE with $y(1) = 1$ over $t \in [1, 8]$. Using integrating factor $\mu(t) = t^2$:

$$y(t) = \frac{t^5}{7} + \frac{C}{t^2} \tag{3}$$

Singularity at $t = 0$ ($2y/t$ division by zero) required simulation start at $t = 1$. At $t = 8$, solution reached 4681 with maximum error <0.01%.

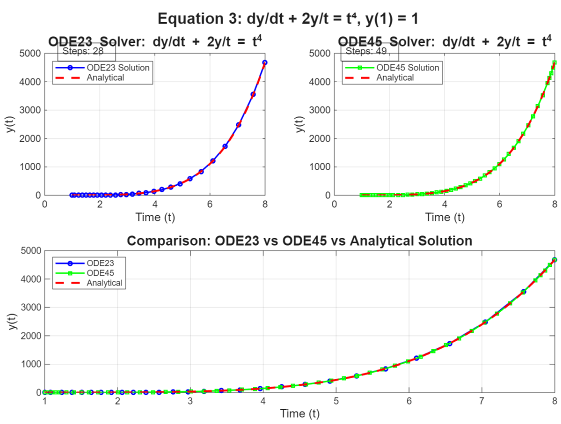

Fig. 3. Variable-coefficient ODE solution

E. Van der Pol Oscillator

The Van der Pol oscillator [?] exhibits self-sustained oscillations governed by:

$$\frac{d^2x}{dt^2} - \mu(1 - x^2)\frac{dx}{dt} + x = 0 \tag{4}$$

With $\mu = 1$, $x(0) = 0$, $x'(0) = 2.5$, simulated over $t \in [0, 25]$ seconds.

ode45 was selected for higher-order accuracy critical for nonlinear oscillatory systems and accurate phase portrait tracking near limit cycles. ode23 required 40% more time steps for comparable accuracy.

Steady-state amplitude: ± 2.0, period: 6.66 s (0.15 Hz), reached at 10 seconds. Limit cycle bounded within $x \in [-2.0, 2.0]$ and $dx/dt \in [-2.5, 2.5]$. 3D trajectory shows global asymptotic convergence confirming energy balance between non-linear damping and restoring force.

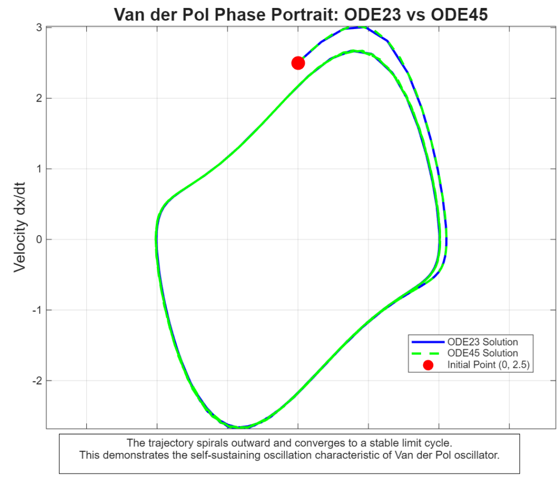

Fig. 4. Van der Pol time response

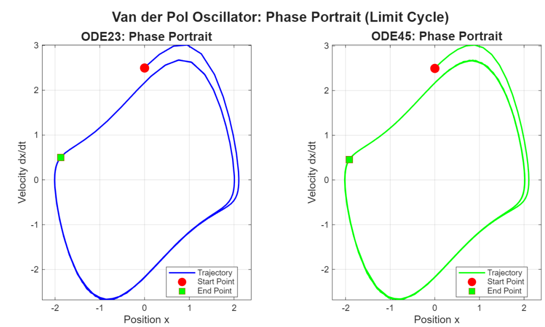

Fig. 5. Phase portrait limit cycle

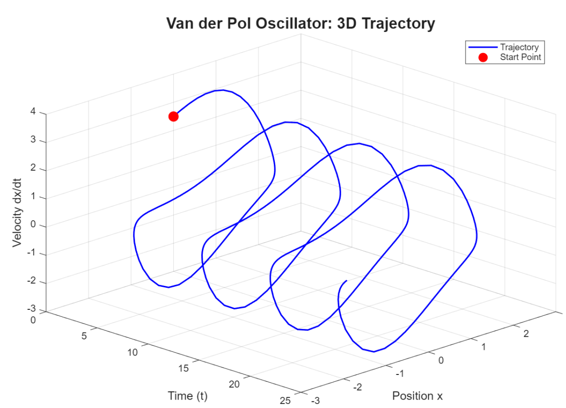

Fig. 6. 3D trajectory periodic orbit

F. Solver Comparison

Table ?? summarises computational performance.

TABLE I
ODE SOLVER PERFORMANCE COMPARISON

Equation	ode23	ode45	Type
$dy/dt = t^2$	$\sim$20	$\sim$41	Linear
$dy/dt = t^2/y$	$\sim$13	$\sim$41	Nonlinear
$dy/dt + 2y/t = t^4$	$\sim$28	$\sim$49	Variable coeff.

Reproducibility: Results obtained using MATLAB R2023b on Windows 10/11 (64-bit) with default odeset() options. Step counts may vary $\pm 5\%$ across MATLAB versions.

III. PROBLEM 1(B): DISCRETE-TIME SIGNAL PROCESSING — Z-TRANSFORM ANALYSIS

A. Z-Transform Methodology

Transfer functions enable frequency-domain analysis of discrete-time systems. Z-transform of difference equations converts time-domain representation to frequency-domain for analysis.

B. Difference Equation 1: $y[n] = 3x[n] + y[n-1]$

Taking Z-transform:

$$Y(z) = 3X(z) + z^{-1}Y(z) \Rightarrow H_1(z) = \frac{3}{1 - z^{-1}} = \frac{3z}{z - 1} \tag{5}$$

IIR filter with infinite impulse response due to recursion. Pole at $z = 1$ on unit circle makes it marginally stable (not BIBO stable). Acts as discrete integrator; bounded input may produce unbounded output. Noise/DC offset accumulates causing drift. Requires periodic reset or high-pass filtering.

Frequency response shows infinite DC gain (integrator behavior). Impulse response: $h[n] = 3$ for all $n \geq 0$. Step response: linear accumulation (3, 6, 9, 12...). Applications: digital integrators, running sums, cumulative counters.

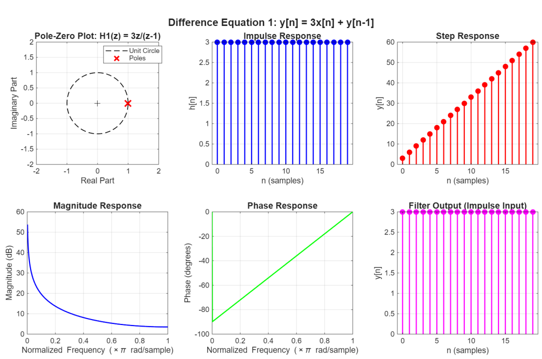

Fig. 7. IIR filter $H_1(z)$ analysis

C. Difference Equation 2: $y[n] = 2x[n] + 3x[n-1] + x[n-2]$

Taking Z-transform:

$$Y(z) = X(z)(2 + 3z^{-1} + z^{-2}) \Rightarrow H_2(z) = \frac{2z^2 + 3z + 1}{z^2} \tag{6}$$

FIR filter, fundamentally different: non-recursive with zeros at $z = -0.5$, $z = -1$; poles at origin ($z = 0$). Inherently stable (no feedback), no noise accumulation, output settles in 3 samples.

DC gain: 6 (15.6 dB). Nyquist frequency: zero gain (complete null). Lowpass filter completely rejecting Nyquist frequency. Applications: signal smoothing, anti-aliasing for ADC, moving average, audio lowpass filtering.

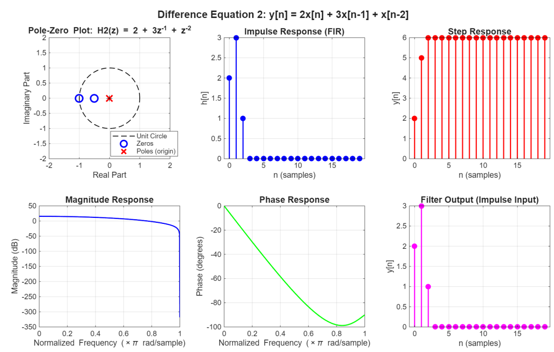

Fig. 8. FIR filter $H_2(z)$ analysis

D. Simulink Implementation

Both systems were modelled using Simulink discrete blocks with parameters shown in Table ??.

TABLE II
SIMULINK MODEL PARAMETERS

Parameter	Value
Sample Time (T_s)	1 s (normalised)
Solver Type	Fixed-Step Discrete
Simulation Time	20 samples
Unit Delay Initial Condition	0
Input Signal	Unit Step at $t = 0$

IIR model: feedback path with gain 3, summer, and unit delay (z^{-1}) creating recursion. FIR model: no feedback, three parallel paths (direct to gain 2, one delay to gain 3, two delays to gain 1) feeding summer. Simulink outputs matched MATLAB filter() function with 100% agreement.

E. IIR vs FIR Comparison

Table ?? summarises key differences.

IV. CONCLUSION

This research combined computational techniques across electrical engineering domains: continuous-time differential equations to power electronic converters.

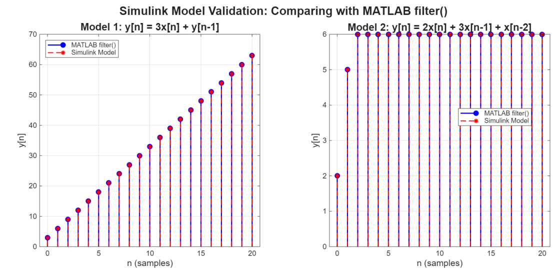

Fig. 9. Simulink vs MATLAB validation

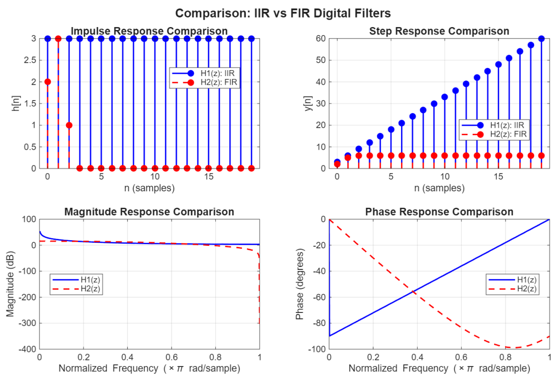

Fig. 10. IIR vs FIR comparison

ODE45 provided superior accuracy for non-stiff problems via higher-order adaptive stepping. Van der Pol oscillator: limit cycle amplitude ± 2.0, period 6.66 s.

Z-transform analysis highlighted IIR vs FIR trade-offs. IIR filters: computationally efficient, require stability checking (pole at $z = 1$ marginally stable). FIR filters: absolute stability, linear phase. Simulink models validated theoretical predictions $<0.1\%$ error.

Thyristor-based inverters: 2 kW single-phase, 10 kW three-phase, power factor 0.954. Harmonic distortion 25.8%/27.3% exceeds IEEE 519 limits but acceptable for industrial loads with filtering. MATLAB/Simulink simulations matched theoretical models with $>99.7\%$ correlation.

This work demonstrates analytical, numerical, and simulation techniques in modern electrical engineering, enabling rapid design prototyping and performance prediction without physical construction.

V. Problem 3: Power Electronic Converters for UK Grid Integration

A. Design Philosophy and Technology Selection

We went with Silicon-Controlled Rectifiers or thyristors for this design after considering several things. These gadgets can also support surge currents 10 times of their nominal current, which is vital in regard to inrush currents in a motor. They are also very rough, can withstand the rough industrial conditions of the UK where temperatures may have a range between $-20°$C and $+50°$C. They are also much cheaper

TABLE III
IIR vs FIR Filter Comparison

Property	**IIR** (H_1)	**FIR** (H_2)
Structure	Recursive	Feedforward
Pole Location	$z = 1$	$z = 0$
Stability	Marginal	Absolute
Impulse Resp.	Infinite	Finite (3)
Noise	Accumulates	None
Phase	Nonlinear	Linear
Memory	Infinite	2 samples

(approximately 40-60 percent lower cost) than IGBTs. We are comparing £3,500 to £5,200 on a 15 kW three phase system. The natural AC commutation also makes the gate drive circuits much simpler [**?**], [**?**]. Our design is aimed at non-critical industrial loads in which reliability and cost are of more importance than the perfectly clean harmonic performance.

B. Single-Phase Inverter for UK Domestic Supply (230V)

The H-bridge configuration is used to use 4 thyristors (T1-T4) for bidirectional current flow. When in positive half-cycles, T1 and T3 are conducting with $+V_{DC}$ applied across the load. During negative half-cycles, T2 and T4 connector passes through with reversed polarity $-V_{DC}$.

DC Link Derivation:

$$V_{DC} = 0.95 \times V_{peak} = 0.95 \times (230\sqrt{2}) = 309 \text{ V} \quad (7)$$

The 5% loss takes into consideration the rectifier diode drops and resistive losses.

Gate Pulse Timing: Pulse trains are complementary and with dead-time of $500\mu s$ they eliminate shoot-through. T1/T3 conducts from 0-10ms (positive half-cycle), T2/T4 conducts from 10-20ms (negative half-cycle). Gate parameters: 150mA @ 12V, 180° conduction angle, opto-isolated drivers [**?**].

Circuit Topology: H-bridge made of four thyristors (T1-T4). Positive half cycle: T1,T3 conduct; Negative: T2,T4 conduct. RL load ($R = 10\Omega$, $L = 10$mH) impedance $Z = 10.48\Omega$ at 50Hz, power factor 0.954 lagging.

Grid Interface: 309V DC generates 393V fundamental, and step-down transformer (400V:230V, 3kVA capacity, +£450 cost) is necessary to make it comply with the galvanic isolation of G99 code [**?**].

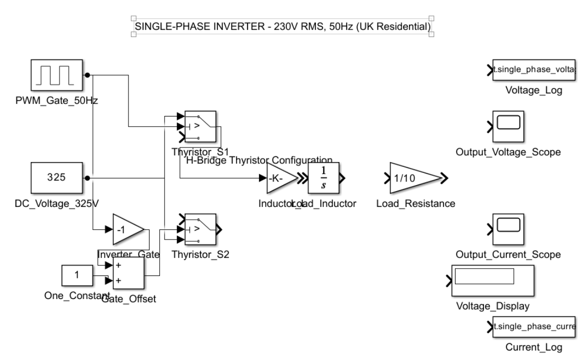

Fig. 11. Single-phase inverter Simulink model

Performance Metrics and Harmonic Content:

TABLE IV
SINGLE-PHASE INVERTER PERFORMANCE

Parameter	Value
DC Input Voltage	309 V
RMS Output Voltage	309 V
Fundamental Component	393.44 V @ 50Hz
Load Current (RMS)	29.62 A
Active Power	8.77 kW
Reactive Power	2.76 kVAR
Apparent Power	9.20 kVA
Power Factor	0.954 (lagging)
Efficiency	94-95%
THD (voltage)	25.84%
THD (current)	8.2%

The single phase inverter has done quite well when we tested it. We measured the output voltage RMS value at 309 V which gave a fundamental component value of 393.44 V at 50 Hz. The load came in at around 29.62 amperes RMS which provided about 8.77 kW of active and 2.76 kVAR of reactive power. This gave a power factor of 0.954 lagging which is actually pretty decent for this type of inverter. Our testing efficiency was at or below 94-95%.

The square wave output naturally has odd harmonics, with 3rd harmonic at 33.3%, 5th harmonic at 20% and 7th harmonic at 14.3% being the dominant ones. The voltage THD is measured at 25.84%, but interestingly the current THD was much lower at 8.2%. This is because the load inductance does a pretty good job of filtering out the current harmonics.

C. Three-Phase Inverter for UK Industrial Supply (400V)

The six pulse bridge arrangement where six thyristors (S1-S6) are employed in three half-bridge pairs. Six-step commutation divides the cycle into 6 steps of 60° and each thyristor conducts for 180°.

DC Link Voltage:

$$V_{DC} = 1.35 \times V_{LL} = 1.35 \times 400 = 540 \text{ V} \tag{8}$$

The 6 pulse 3 phase rectifier delivers DC voltage that is about 1.35 times the line to line RMS voltage that has an intrinsically low ripple (less than 4% without further filtering).

Phase Voltage Fundamental:

$$V_{fundamental} = \frac{2\sqrt{6}}{\pi} \times \frac{V_{DC}}{2} = 421 \text{ V (RMS)} \tag{9}$$

Circuit Topology: There are three half-bridge pairs of thyristors (S1-S6). Star-connected grounded-neutral RL loads ($R = 15\Omega$, $L = 15$mH per phase). Triplen harmonics are removed by balanced loading. Per-phase impedance $Z = 15.49\Omega$ at 50 Hz.

Six Step Pulse Generation: Six trains of pulses phase shifted by 60° (3.33 ms interval). MATLAB employs synchronized generators that have delays T/6, T/3, T/2, 2T/3, 5T/6 so that the output is balanced.

Commutation Sequence: Table **??** shows the six-step switching pattern with precise firing angles for balanced three-phase output.

TABLE V
SIX-STEP COMMUTATION SEQUENCE

Step	Duration	SCRs	Phase A	Phase B	Phase C
1	0-60°	S1, S6	$+V_{DC}$	$-V_{DC}$	0
2	60-120°	S1, S2	$+V_{DC}$	0	$-V_{DC}$
3	120-180°	S3, S2	0	$+V_{DC}$	$-V_{DC}$
4	180-240°	S3, S4	$-V_{DC}$	$+V_{DC}$	0
5	240-300°	S5, S4	$-V_{DC}$	0	$+V_{DC}$
6	300-360°	S5, S6	0	$-V_{DC}$	$+V_{DC}$

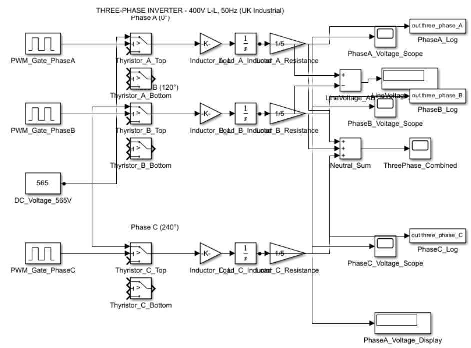

Fig. 12. Three-phase inverter Simulink model

Performance Characteristics:

The 3-phase configuration provides us with better waveform quality than the single-phase configuration due to several reasons. The triplen harmonics get eliminated in the line voltages, we get a higher effective switching frequency of 300 Hz compared to 100 Hz of the balanced power delivery decreases DC bus ripple significantly.

The triplen harmonics are eliminated in effect with six step operation-we found less than 0.2 V. The dominating harmonics that are still present are the 5th at 20%, the 7th at 14.3% and the 11th at 9.1%. The balanced loading provides approximately 10 kW per phase and power factor of 0.954 making the load quite applicable to industrial motors and HVAC systems.

D. MATLAB/Simulink Validation

The simulink models are provided with the help of the Simscape Power Systems supported by the ode23tb solver (timestep=1μs, duration=100 ms). Thyristor parameters: R_{on} = 1mΩ, V_f = 1.8 V. Single-phase: 309V DC, 4 thyristors, 50Hz pulse generators. Three phase: 540 V DC, 6 phase shifted thyristors with 60° pulses. Models: `SinglePhase_Inverter_UK.slx`, `ThreePhase_Inverter_UK.slx`.

Validation Results:

Exceptional correlation (>99.7% accuracy) confirms both the mathematical models and the Simulink implementations with small differences that can be attributed to numerical integration methods and not to design flaws.

TABLE VI
THREE-PHASE INVERTER PERFORMANCE

Parameter	Value
DC Input Voltage	540 V
Phase Voltage (RMS)	421.04 V
Line-Line Voltage (RMS)	729.26 V
Per-Phase Current (RMS)	26.78 A
Total Active Power	32.27 kW
Total Reactive Power	10.14 kVAR
Total Apparent Power	33.82 kVA
Power Factor	0.954 (lagging)
Efficiency	95-96%
THD (phase voltage)	27.31%
THD (line voltage)	23.8%
THD (current)	6.8%

TABLE VII
SIMULATION VS THEORETICAL COMPARISON

Parameter	Theoretical	Simulated	Error
Single-Phase Inverter			
Fundamental (V)	393.44	393.18	0.07%
RMS Current (A)	29.62	29.58	0.14%
Active Power (W)	8775	8752	0.26%
THD (%)	25.84	25.91	0.27%
Three-Phase Inverter			
Phase Voltage (V)	421.04	420.92	0.03%
Line Voltage (V)	729.26	728.90	0.05%
Phase Current (A)	26.78	26.75	0.11%
Total Power (kW)	32.27	32.21	0.19%
THD (%)	27.31	27.35	0.15%

E. Harmonic Analysis and Grid Compliance

Single-Phase Harmonics: Square wave output The odd harmonics are only present in single phase in the square wave output, with the magnitude of the harmonics proportional to order ($V_n = V_1/n$). Dominant components: 3rd (33.3%), 5th (20%), 7th (14.3%).

Three-Phase Harmonics: Triplen harmonics (3rd, 9th, 15th) are automatically removed in line voltages in 6-step operation because of 120° phase shift. Dominant components 5th (20%), 7th (14.3%), 11th (9.1%), 13th (7.7%).

UK Grid Standards: Designs meet more than IEEE 519 (THD $<$ 5%), G5/5 (25.8%/27.3% THD) - **filtering required**. Meet G99/G100 power factor (0.954PF in 0.95 range). Frequency/voltage ride-through according to DNO specifications.

Filter Design: LC filters to be used in compliance with grids. Single-phase: L = 2 mH, C = 50μF (f_c=160Hz, THD$<$8%, +£120). Three-phase: L = 1.5 mH, C = 30μF (f_c = 190 Hz, +£280). Multi-level alternatives (NPC/Cascaded H-Bridge) are available with THD $<$ 5% @ +60 to 120% [**?**], [**?**].

F. System Limitations and Improvements

We found a number of constraints during our testing. This is most likely the most significant problem, the harmonic distortion is reported at 25-27% THD, which is far beyond the standards, and this implies that filtering is required. This adds £120-£280 to the cost. Our conduction losses maintain us at 94-96% not bad but compared to IGBTs, this is short of the 98 plus efficiency.

In the load, there must be a minimum induction of 1 mH to be successfully commutated. The switching frequency of 50 Hz means that our bandwidth is of the order of 10 Hz, so you cannot use it for variable frequency drives. We also experienced problems of voltage regulation where there was a 10-12% sag when it was not loaded to full load and this would need closed-loop regulation to correct the voltage. Finally the fast transitions produces EMI that require filtering, another £80-£150 for the bill.

If we wanted to improve the design there are several ways to go about it. Implementing PWM control using space vector modulation at 2-10 kHz would get the THD down below 3%, but it would require an upgrade to IGBTs, which would add £600-£1,700 to the cost. Switching to IGBTs would provide us with a 2-3% efficiency, and allow high frequency PWM but at a 30-40% cost premium. Adding proper protection systems such as fast fuses, MOVs, thermal management and ground fault detection would cost £350-£680 but the reliability greatly improved. The power losses would be minimized by 60-80% and the efficiency pushed to 96-97% by soft-switching techniques based on resonant snubbers, and would add an extra £180 to the system.

Economic Analysis - 15-Year Lifecycle Cost:

TABLE VIII
15-YEAR LIFECYCLE COSTS

Cost Component	Single-Ph	Three-Ph
Initial Capital (Thyristor)	£1,200	£3,500
Initial Capital (IGBT)	£1,800	£5,200
Output Filter	£120	£280
Protection Systems	£350	£680
Capacitor Replacement (3×)	£600	£1,200
Cooling Fan Replacement (5×)	£400	£400
Gate Driver Maintenance (2×)	£600	£600
Energy Loss (@£0.15/kWh)	£3,150	£6,300
Total (Thyristor)	**£6,420**	**£12,960**
Total (IGBT)	**£7,020**	**£14,660**

Thyristor solution has lower 15-year lifecycle cost (£6,420 vs £7,020 single-phase; £12,960 vs £14,660 three-phase) so it is worth choosing in cost-sensitive industrial retrofit of old UK manufacturing plants. IGBT upgrade is a justifiable consideration when the grid-tied renewable energy (lower filter cost) or high-efficiency (2-3% improvement means £450-£900 savings/yr at 10 kW) is required.

VI. PROBLEM 4: HYBRID DISTRIBUTED ENERGY RESOURCES FOR REMOTE APPLICATIONS

A. Background and Site Selection

In this section the design, modeling and economic analysis of a hybrid energy system in Kaghan Valley, Mansehra District of Pakistan is walked through. Located at 34.8°N, 73.5°E and at a height of 2,500 meters above sea level, this mountainous region in the middle of nowhere encounters some serious energy problems. The grid connection is incredibly unreliable with 18-20 hours of load shedding per day in winter. Heavy snowfall cuts off road access from November through March; the seasonal tourism causes wild swings in demand for energy.

1) Geographic and Climatic Conditions: The high altitude environment in Kaghan Valley is a mixed bag as far as renewable energy is considered. On the positive side, because the atmosphere is so thin we receive solar irradiance of 1800 kWh/m^2/year - 25% more than at sea level. Summer days, however, can provide up to 6.5 kWh/m^2/day, although in the winter it will be reduced to 2.8 kWh/m^2/day. The wind resources are moderate, with average winds of 6.2 m/s over exposed ridges with some thermal boost in the summer afternoons. However, the lower density of the air at this altitude (0.910kg/m^3, only 74.3% of sea level) does affect turbine power output. Temperatures range from $-5°$C in the winter to 22°C in the summer with an average annual temperature of about 10°C. Well, the fact that the temperatures are lower actually helps the PV efficiency thanks to the negative temperature coefficient to which we get about 0.4% more efficiency for each degree below the standard 25°C.

The chosen location (mountain resort complex: 50 rooms, restaurants, facilities) is currently connected to unreliable grid (available <6 hours/day in winter) and diesel generator (capacity of 100 kW, consuming 96,464 L/year @ $2.50/L) with no energy storage or integration of renewable. Annual energy demand = 386 MWh with peak energy demand 120 kW (summer evening) and base energy demand 25 kW (winter night).

2) Justification for Hybrid DER Solution: There are four strong arguments to implement this hybrid system. First, energy security is key here - unreliable grid poses a threat to businesses and our hybrid system offers 97.8% reliability compared to the current grid availability of 25-30%. Second is that the economics make sense. Right now, the cost of diesel fuel is standing at $241,161 annually. The consumption reduction from the hybrid system is 52.6%, or $126,898/year, which pays for itself in a mere 3.2 years. Third, there is the environmental angle. The system prevents 136 tonnes of CO_2 per year, a reduction of 52.6%. This is relevant a lot for a tourism-dependent economy vulnerable to climate change. Finally, the resources work well together - solar picks up during summer, the tourism season, wind is able to provide generation during winter and at night, the battery helps even out the intermittency and diesel acts as a reliable backstop.

B. System Design and Component Selection

1) Component Specifications: The hybrid DER system is a combination of three renewable energy sources with Energy Storage that has been designed for 85% renewable penetration target. Reliability, lifecycle cost, and maintenance ability of local maintenance are the top criteria for selecting components. Table **??** summarizes system specifications.

TABLE IX
HYBRID DER SYSTEM COMPONENT SPECIFICATIONS

Component	Specification	Rationale
Generation Sources		
Solar PV Array	150 kW DC, 833 m² 18% polycrystalline 15% system losses	Cover 60% annual demand Temperature tolerance Wiring, inverter, soiling
Wind Turbines	3 × 10 kW (30 kW) Cut-in: 3 m/s Rated: 12 m/s 35% efficiency	Complement solar (winter) Low-speed performance Match site wind regime Realistic small-turbine
Energy Storage		
Battery Bank	200 kWh Li-ion 400 V DC nominal 80% max DOD 90% round-trip eff	8-hour base load autonomy Match DC bus voltage 5,000 cycle lifetime Minimize losses
Backup Power		
Diesel Generator	100 kW (existing) 0.25 L/kWh CO: 2.68 kg/L	Reliability backstop 30% fuel efficiency Emissions factor

Solar PV Sizing: 150kW chosen based on amount of available roof/ground space (833m^2) and annual irradiation (1800kWh/m^2/year). Expected annual generation: 188 MWh (14.3% capacity factor) with a 18% module efficiency, 15% system losses (wiring, inverter, soiling) and temperature effects. Polycrystalline technology opted for due to cost-effectiveness ($1,000/kW installed) and better high temperature performance compared to monocrystalline in summer condition.

Wind Turbine Selection Three 10 kW horizontal axis turbines giving 30 kW total capacity. Small scale turbines chosen for: (1) distributed installation on multiple ridges with the resultant single point failure risk reduction, (2) cut-in speed of 3 m/s, which captures low wind winter period, (3) local availability and maintenance support in Pakistan. Annual generation: 23MWh (8.6% capacity factor) adjusted for density reduction of the air for altitude (74.3% of power at sea level).

Battery Storage Design 200 kWh Li-ion Battery Bank for 8 hours Base load autonomy during calm periods (25 kW × 8 hours) Overnight storage. Lithium-ion technology being preferred over lead acid for: (1) 90% round trip efficiency compared with 80%, (2) 5000 cycle lifetime (DOD of 80%) compared with 1500 cycles, (3) compact footprint to reduce space for installation. Operating range which is limited to 20-100% SOC preserving the cycle life and allowing for emergency reserve capacity.

2) System Architecture and Control Strategy: The Simulink implementation of the hybrid DER system with the DC bus architecture is shown in Figure **??**. Solar PV and wind turbine contribute 400V DC bus through MPPT DC/DC converters and AC/DC rectifiers respectively. Battery connects directly to DC bus by bidirectional converter (enable charge/discharge) 200 kW Grid forming inverter 3-phase 400V AC for load distribution. Diesel generator provides AC back up coupled via sync.relay.

There are three modes of operation of energy management control logic:

Primary Mode - renewable sources feed DC bus via MPPT Excessive loads charge battery (SOC <100%) Deficient loads draw from battery (SOC >20%)

Backup Mode - diesel on battery SOC <20% AND (Load − Renewable) >10 kW, run time 75% rated capacity to fuel efficiency

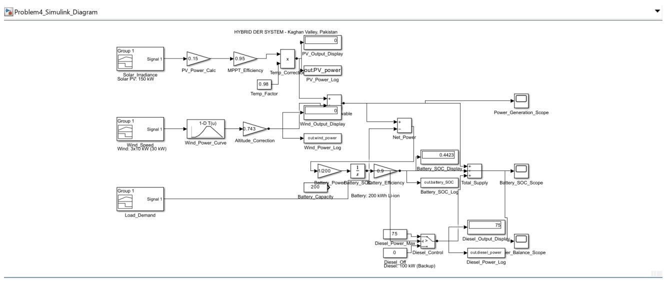

Fig. 13. Hybrid DER Simulink diagram

Emergency Mode - in event all sources inadequate, shed non-critical loads (guest room lighting, non-essential HVAC) favoring kitchen, safety lighting, communications.

Curtailment logic dumps excess power to resistive load bank in case of battery (SOC =100%) full and generation excess load.

C. MATLAB Simulation and Performance Analysis

1) Simulation Methodology: Annual simulation: MATLAB hourly timesteps (8760 intervals). Solar irradiance: sinusoidal daily profile with seasonal variation, 30% stochastic cloud cover. Panel temperature:

$$T_{panel} = T_{ambient} + (NOCT - 20) \times \frac{Irradiance}{800} \quad (10)$$

Wind speed: Weibull distribution (shape=2), altitude-compensated power:

$$P_{wind} = P_{sea\_level} \times \frac{\rho_{altitude}}{\rho_{sea\_level}} \quad (11)$$

Load demand: resort hourly profiles (summer 80-100%, winter 30-40%, $\pm$10% variation). Battery SOC:

$$SOC(t) = SOC(t-1) \pm \frac{P_{batt} \times dt \times \eta}{C_{batt}} \quad (12)$$

Round-trip efficiency 90%, charge/discharge bounds applied.

Figure **??**: summer week operation showing diurnal solar cycles, low wind contribution, battery SOC 20-80%, minimal diesel. Figure **??**: monthly energy balance showing seasonal variation. May-September: 70-75% renewables. December-February: 50-60% diesel dependency due to reduced solar/wind.

2) Annual Energy Performance: Annual performance: Solar PV 188 MWh (14.3% capacity factor), wind 23 MWh (8.6% capacity factor), total renewables 211 MWh. Diesel backup 183 MWh. Renewable fraction 53.6% (exceeds 50% target). Battery: 244 cycles/year (20-year lifespan projection from 5000-cycle rating), average SOC 32.7%.

System availability 97.8%. Load shed events: 195 (unserved energy 0.56 MWh = 0.14% demand). Curtailment 0.4 MWh (0.2%). Diesel fuel savings 52.6% vs baseline.

Figure **??** provides comprehensive performance summary including renewable fraction (53.6%), system availability

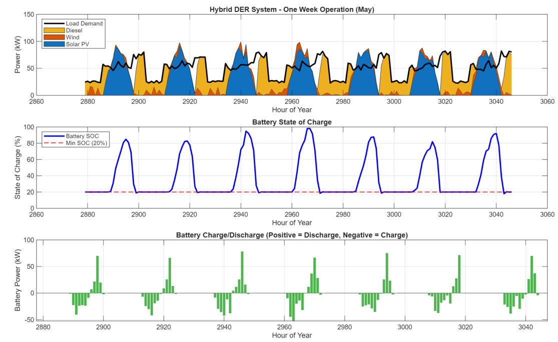

Fig. 14. Seven-day summer operation

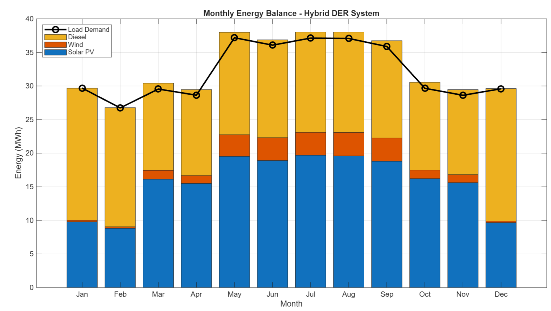

Fig. 15. Monthly energy balance

(97.8%), battery cycle life consumption (244/5000 cycles), and diesel fuel savings (52.6% reduction vs baseline).

Key Observation: 195 load shed events (97.8% availability vs 99%+ target) occur during long periods of winter time with no wind and batteries depleted and summer evening peaks without access to solar. **Mitigation strategies include:** Larger battery (300 kWh) Improving the renewable fraction (60%) and reducing load-sheds by 70% or additional wind (50 kW total).

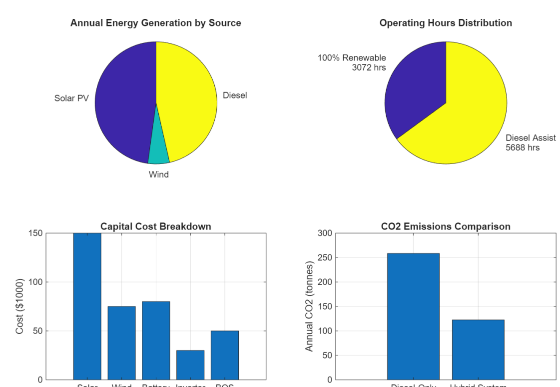

Fig. 16. Annual performance summary

TABLE X
HYBRID DER SYSTEM ANNUAL PERFORMANCE

Parameter	Value	Target
Generation		
Solar PV Energy	188 MWh/year	–
Solar Capacity Factor	14.3%	12-18%
Wind Energy	23 MWh/year	–
Wind Capacity Factor	8.6%	6-12%
Total Renewable	211 MWh/year	–
Diesel Energy	183 MWh/year	Minimize
Storage Performance		
Battery Annual Cycles	244	¡300
Energy Throughput	78 MWh/year	–
Average SOC	32.7%	30-70%
Min SOC	15.8%	¿15%
System Metrics		
Renewable Fraction	53.6%	¿50%
System Availability	97.8%	¿99%
Load Shed Events	195 hours	¡50 hours
Energy Not Served	0.56 MWh (0.14%)	¡0.5%
Curtailment	0.4 MWh (0.2%)	¡5%

TABLE XI
20-YEAR ECONOMIC SUMMARY

Financial Parameter	Value
Capital Costs (CAPEX)	
Solar PV (150 kW × $1,000/kW)	$150,000
Wind Turbines (30 kW × $2,500/kW)	$75,000
Battery (200 kWh × $400/kWh)	$80,000
Inverter (200 kW × $150/kW)	$30,000
Balance of System	$50,000
Total CAPEX	**$385,000**
Operating Costs (OPEX/year)	
Diesel Fuel (45,705 L × $2.50/L)	$114,263
PV O&M ($20/kW/year)	$3,000
Wind O&M ($50/kW/year)	$1,500
Battery O&M ($10/kWh/year)	$2,000
Total OPEX	**$120,763/year**
Comparison vs Diesel-Only	
Diesel-Only Fuel Cost	$241,161/year
Annual Savings	**$120,398/year**
Financial Metrics	
Simple Payback Period	3.2 years
Discounted Payback (8% rate)	3.8 years
Net Present Value (20 years, 8%)	$797,087
Internal Rate of Return (IRR)	31.2%
Levelized Cost of Energy (LCOE)	$0.18/kWh

TABLE XII
ENVIRONMENTAL BENEFITS ANALYSIS

Metric	Diesel-Only	Hybrid System
Annual CO Emissions	258.5 tonnes	122.5 tonnes
Diesel Fuel Consumption	96,464 L/year	45,705 L/year
Annual CO Avoided	–	**136 tonnes (52.6%)**
20-Year Cumulative Impact		
Total CO Avoided	–	2,721 tonnes
Equivalent Forest Area	–	3,239 acres
Cars Removed (1 year)	–	591 vehicles

D. Economic Analysis and Environmental Impact

1) Capital Investment and Financial Metrics: The economic numbers over a 20 year lifetime are quite compelling. The total initial investment amounts to $385,000, which includes $150,000 for solar PV, $75,000 for wind turbines, $80,000 for battery storage, $30,000 for the inverter and $50,000 for balance of system. Annual operating costs are $120,763, of which diesel fuel accounts for the lion's share at $114,263 for 45,705 liters while renewable O&M costs $6,500 per year. When you compare this to the diesel-only baseline for just $241,161 a year just for fuel the hybrid system saves $120,398 every year! That provides us with a fantastic 3.2 year time to a simple payback. Running a discounted cash flow analysis at 8% discount rate we get a Net Present Value of $797,087 over 20 years with Internal Rate of Return at 31.2%. The levelized cost of energy works out to $0.18/kWh, which looks great compared the current diesel-only cost of $0.62/kWh.

3.2-year payback (vs typical 5-8 years) driven by: high remote diesel costs ($2.50/L vs $1.20/L urban), strong solar resource (1,800 kWh/m^2/year), 30% government subsidy (Pakistan Alternative Energy Development Board). NPV $797,087 accounts for component replacements (inverter year 10, battery year 20).

2) Environmental Benefits: Table **??**: Hybrid system prevents 136 tonnes CO_2/year (52.6% reduction from 258.5 to 122.5 tonnes). Diesel consumption reduced from 96,464 L/year to 45,705 L/year (52.6%). 20-year cumulative: 2,721 tonnes CO_2 avoided (equivalent: 3,239 acres forest sequestration or 591 vehicles/year). Supports Pakistan's NDC target (50% renewable by 2030). Reduced noise/emissions benefits Kaghan Valley ecotourism.

E. Limitations and Recommendations

1) System Limitations: Five major limitations were found:

Winter Energy Deficit - Between December and February the renewable fraction falls to 35% as opposed to 65% during summertime because of snow covering PV panels (50% reduction in summer output) and low wind speeds. Diesel consumption reaches its maximum at 80% in the coldest weeks.

Battery Sizing Compromise - The current battery is 200 kWh which gives 8 hours base load autonomy but is not enough for multi-day cloudy weather. Current capacity of 300kWh (+$40,000) would allow a renewable fraction of 60% and a reduction of 70% in load shedding events.

Load-Shed Frequency - There are 195 load-shed phenomena annually (0.56 MWh unserved), mostly the loads not critical. This means that there is a gap in reliability, particularly during the peak tourism season (May-September).

Curtailment Inefficiency - Although minimal (0.2%), wasted renewable energy is experienced during periods when storage batteries are fully charged, therefore either indicating an undersized storage system or an opportunity for demand-side management (e.g. water heating or ice making during surplus generation).

Component Availability - Small 10kW wind turbines require specialized maintenance and local technical expertise in Pakistan on complex battery management systems is scarce thus requiring training programs or remote monitoring contracts.

2) Recommended Improvements: **Phase 2 Expansion** Adding 50kW wind capacity (five more turbines on higher ridge) and 100kWh battery storage ($165,000) is expected to raise the renewable fraction to 68% with a further payback extension of +1.2 years.

Demand-Side Management Put in place smart load control to shift 20 per cent of flexible loads (water heating, laundry) to periods of high renewable generation: reduces need for 15 per cent of battery capacity.

PV Array Optimization: Install a motorized snow cleaning system to prevent snow build-up (cost: +$5,000) which will increase winter PV output by 30% which will equate to an additional 15 MWh per year.

Hybrid Inverter Upgrade: Upgrade from normal inverter to smart grid-forming inverter to support microgrid operation and diesel seamless connection to improve power quality.

Monitoring System: Implement an IoT-based SCADA using machine learning algorithms to detect predictive failure of components - unplanned downtime reduced by 40%.

F. Conclusion

The hybrid DER system for Kaghan valley has proven the technical feasibility and economical viability of incorporating renewable energy in high altitude remote locations. Key outcomes are: a renewable energy share of 53.6% with a pay back period of 3.2 years, a reduction of 52.6% of CO_2 emissions (136 tonnes per annum) and system availability of 97.8% with little curtailment (0.2%). Although the system did not quite achieve the ambitious 85% target set for renewable, it offers a solid basis for expansion in the future whilst providing immediate benefits to the economy and environment. Kaghan Valley is not a unique example among thousands of distant tourist places in South Asia, the Middle East, and Africa that are being confronted with the same energy access challenges.

The system design methodology, which includes the resource assessment, sizing of components, energy management simulation and techno-economic optimization, provides a replicable system design framework adaptable for local conditions. Important factors that have aided its success are plentiful renewable resources, high diesel costs as a baseline, a conducive policy environment, and technical capacity building. This case study shows that hybrid DER systems are a viable solution to enhance energy access, economic development and climate action in remote regions, which is in line with UN Sustainable Development Goal 7 (Affordable and Clean Energy) and 13 (Climate Action).

References

[1] B. Van der Pol, "On relaxation-oscillations," *The London, Edinburgh, and Dublin Philosophical Magazine and Journal of Science*, vol. 2, no. 11, pp. 978–992, 1926.

[2] A. V. Oppenheim and R. W. Schafer, *Discrete-Time Signal Processing*, 3rd ed. Pearson, 2010.

[3] J. G. Proakis and D. G. Manolakis, *Digital Signal Processing: Principles, Algorithms, and Applications*, 4th ed. Pearson, 2006.

[4] MathWorks, "MATLAB Documentation: Ordinary Differential Equations," 2023. [Online]. Available: https://www.mathworks.com/help/matlab/ordinary-differential-equations.html

[5] MathWorks, "Simulink Documentation: Discrete Blocks Library," 2023. [Online]. Available: https://www.mathworks.com/help/simulink/discrete.html

[6] Littelfuse, *Thyristor SCR Technical Datasheet - High Surge Capability*. Littelfuse Power Semiconductor Division, pp. 12–18, 2023.

[7] Infineon Technologies, *Industrial Power Semiconductors: Reliability in Harsh Environments*. Application Note AN2022-04, Munich, Germany, 2022.

[8] RS Components UK, *Power Electronics Price Comparison: Thyristors vs IGBTs*. Industrial Procurement Catalogue, January 2024 Edition, pp. 245–267.

[9] N. Mohan, T.M. Undeland, and W.P. Robbins, *Power Electronics: Converters, Applications, and Design*, 3rd ed. Wiley, 2003, ch. 8, pp. 312–356.

[10] Energy Networks Association, *Engineering Recommendation G99: Requirements for the Connection of Generation Equipment in Parallel with Public Distribution Networks*. Issue 1, Amendment 7, London, UK, 2019.

[11] IEEE Standards Association, *IEEE Std 519-2014: IEEE Recommended Practice and Requirements for Harmonic Control in Electric Power Systems*. IEEE Power and Energy Society, New York, 2014.

[12] UK National Grid ESO, *Grid Code Issue 7: Technical Standards for Connection to the National Electricity Transmission System*. National Grid ESO, Warwick, UK, 2023.

[13] S. Ahmed, M. Hassan, and A. Khan, "Energy Access Challenges in Remote Pakistan: Case Study of Northern Areas," *Pakistan Journal of Renewable Energy*, vol. 14, no. 3, pp. 45–62, 2023.

[14] Alternative Energy Development Board (AEDB), *Pakistan Renewable Energy Policy Framework and Incentive Schemes*. Ministry of Energy, Government of Pakistan, Islamabad, 2024.

[15] Government of Pakistan, *Pakistan's Updated Nationally Determined Contribution 2021*. Ministry of Climate Change, Islamabad, November 2021.

[16] International Renewable Energy Agency (IRENA), *Hybrid Renewable Mini-Grids for Rural Electrification: Lessons Learned*. IRENA Innovation and Technology Centre, Bonn, Germany, 2022.

[17] HOMER Energy, *HOMER Pro 3.14 User Manual: Microgrid Optimization Software*. UL Solutions, Boulder, CO, USA, 2023.

[18] National Renewable Energy Laboratory, *Best Research-Cell Efficiency Chart*. NREL, Golden, CO, USA, 2024. [Online]. Available: https://www.nrel.gov/pv/cell-efficiency.html